Electronic Supplementary Information

Two isomeric metal-organic frameworks bearing stilbene moieties for high volatile iodine uptake

Jianping Tang,‡[ac] Shenghua Zhou,‡[ab] Mengyi Huang,[ad] Zhenxin Liang,[a] Shaodong Su,[a] Yuehong Wen,*[ab] Qi-Long Zhu,[ab] and Xintao Wu[ab]

[a] State Key Laboratory of Structural Chemistry, Fujian Institute of Research on the Structure of Matter, Chinese Academy of Sciences, Fuzhou 350002, China
[b] University of Chinese Academy of Sciences, Beijing 100049, China
[c] College of Chemistry, Fuzhou University, Fuzhou, 350002, China
[d] College of Chemistry and Materials Science, Fujian Normal University, Fuzhou 350007, China

*Corresponding Authors. E-mail: yhwen@fjirsm.ac.cn

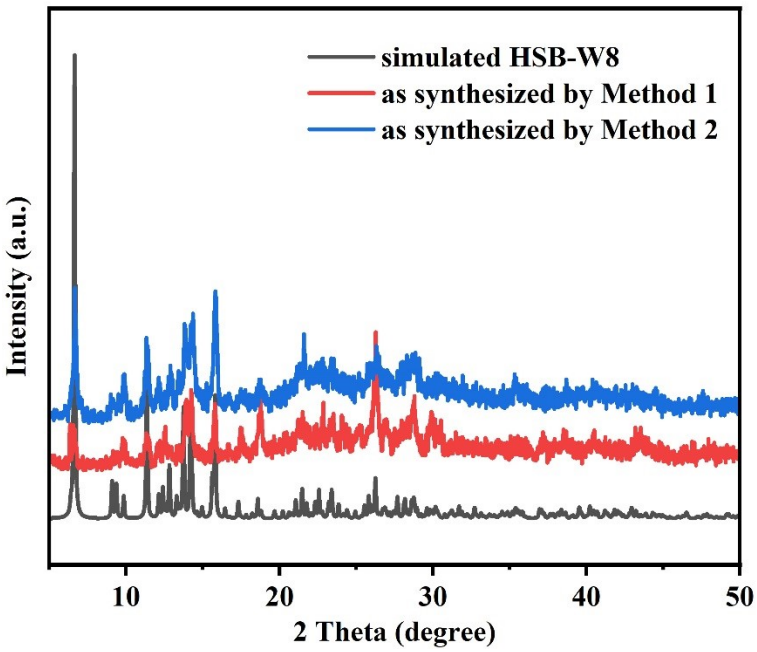

Fig. S1 PXRD patterns of HSB-W8 prepared by different methods.

Table S1. Crystallographic data and refinement details for HSB-W8 and HSB-W9.

Name	HSB-W8	HSB-W9
Empirical formula	$C_{31.5}H_{31.5}N_{4.5}O_{4.5}Cd$	$C_{30}H_{28}N_4O_4Cd$
M	657.51	620.96
Crystal system	triclinic	monoclinic
Space group	*P*-1	*C*2/c
a (Å)	9.045(4)	14.841(2)
b (Å)	13.372(6)	12.6145(14)
c (Å)	13.841(7)	18.084(2)
α (°)	87.814(12)	90
β (°)	85.762(10)	105.677(13)
γ (°)	84.392(10)	90
V/Å^3	1660.7(13)	3259.6(7)
Z	2	1
ρ_{calc} (g/cm^{-3})	1.315	0.316
μ/mm^{-1}	0.698	0.959
$2\theta_{range}$(°)	5.71 to 52.77	8.128 to 123.26
h, k, l, ranges	-11 to 11, -13 to 16, -17 to 16	-18 to 19, -16 to 16, -22 to 23
F(000)	672.0	316.0

R1,[a]wR$_2$[b][I>2σ(I)]	0.0621, 0.1698	0.1095, 0.2573
GOF on F^2	1.052	1.150

[a] $R = \Sigma(||Fo| - |Fc||)/\Sigma|Fo|$. [b] $Rw = \{\Sigma w[(Fo^2 - Fc^2)^2]/\Sigma w[(Fo^2)^2]\}^{1/2}$.

Table S2. Selected bond lengths (Å) and angles(°) of HSB-W8.

Cd[a]-N1[b]	2.402(5)
Cd[a]-N2[a]	2.392 (4)
Cd[a]-N3[a]	2.427(5)
Cd[a]-N4[c]	2.383 (5)
Cd[a] -O1[a]	2.258(4)
Cd[a]-O2[a]	2.262(4)
N1[b]-Cd[a]-O1[a]	85.47(17)
N1[b]-Cd[a]- O2[a]	92.06 (18)
N1[b]-Cd[a]- N2[a]	99.15 (16)
N1[b]-Cd[a]-N3[a]	171.69(15)
N1[b]-Cd[a]-N4[c]	81.30(16)
N2[a] -Cd[a]-O1[a]	95.06(17)
N2[a] -Cd[a]- O2[a]	88.99(17)
N2[a] -Cd[a]-N3[a]	77.07(16)
N2[a] -Cd[a]-N4[c]	173.83(15)
N3[a]-Cd[a]-O1[a]	87.49(17)
N3[a]-Cd[a]- O2[a]	95.26(18)
N3[a]-Cd[a]-N4[c]	103.27(17)
N4[c]-Cd[a]-O1[a]	91.11(17)
N4[c]-Cd[a]- O2[a]	84.84(17)
O1[a]-Cd[a]- O2[a]	175.54(16)

Symmetry codes: (a) x, y, z; (b) 1-x, -y, 2-z; (c) 1-x, -y, 1-z.

Table S3. Selected bond lengths (Å) and angles(°) of HSB-W9.

Cd[a]-N1[a]	2.337(7)
Cd[a]-N2[b]	2.377 (7)
Cd[a]-N3[c]	2.377(8)
Cd[a]-N4[d]	2.337 (7)
Cd[a] -O1[d]	2.287(7)

Cd^{a}-$O2^{a}$	2.287(7)
$N1^{a}$-Cd^{a}-$O1^{d}$	87.8(3)
$N1^{a}$-Cd^{a}- $O2^{a}$	90.2(3)
$N1^{a}$-Cd^{a}- $N2^{b}$	95.0(3)
$N1^{a}$-Cd^{a}-$N3^{c}$	171.0(3)
$N1^{a}$-Cd^{a}-$N4^{d}$	93.8(4)
$N2^{b}$ -Cd^{a}-$O1^{d}$	87.8(3)
$N2^{b}$ -Cd^{a}- $O2^{a}$	94.6(3)
$N2^{b}$ -Cd^{a}-$N3^{c}$	76.4(4)
$N2^{b}$ -Cd^{a}-$N4^{d}$	171.0(3)
$N3^{c}$-Cd^{a}-$O1^{d}$	94.6(3)
$N3^{c}$-Cd^{a}- $O2^{a}$	87.8(3)
$N3^{c}$-Cd^{a}-$N4^{d}$	95.0(3)
$N4^{d}$-Cd^{a}-$O1^{d}$	90.2(3)
$N4^{d}$-Cd^{a}- $O2^{a}$	87.8(3)
$O1^{d}$-Cd^{a}- $O2^{a}$	177.0(4)

Symmetry codes: (a) x, y, z; (b) 0.5-x, 0.5+y, 1.5-z; (c) 0.5+x, 0.5+y, z; (d) 1-x, y, 1.5-z.

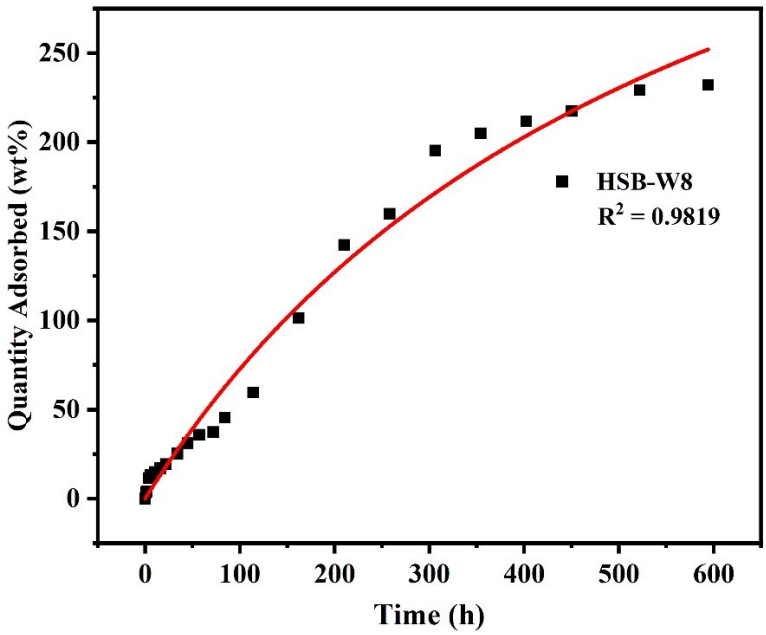

Fig. S2 Pseudo-second-order kinetic curves of I_2 adsorption on HSB-W8 at 25 °C.

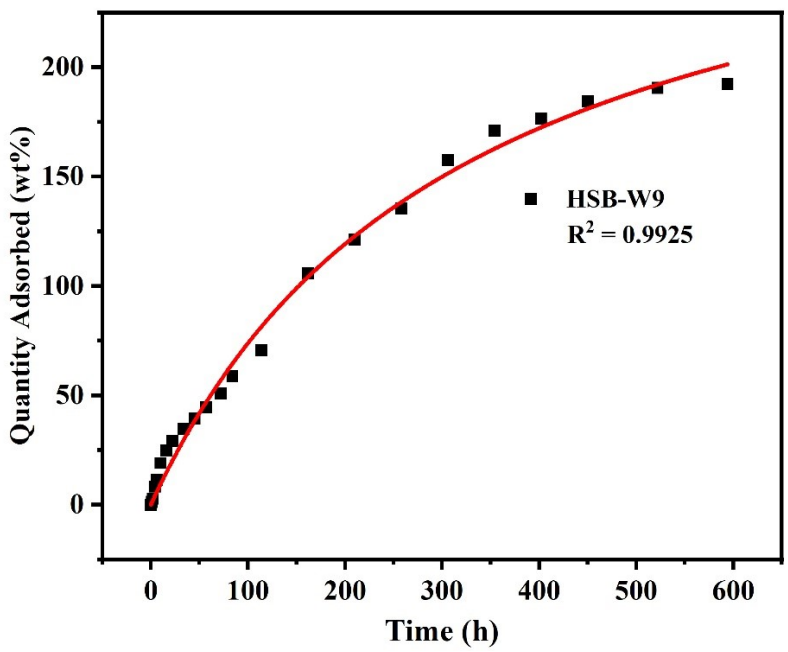

Fig. S3 Pseudo-second-order kinetic curves of I_2 adsorption on HSB-W9 at 25 ℃.

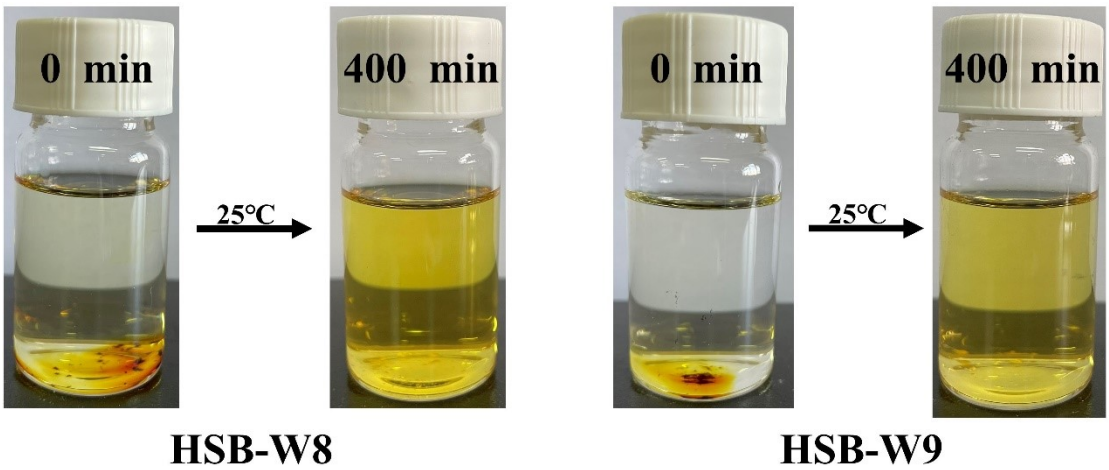

Fig. S4 The change of the iodine solution color.

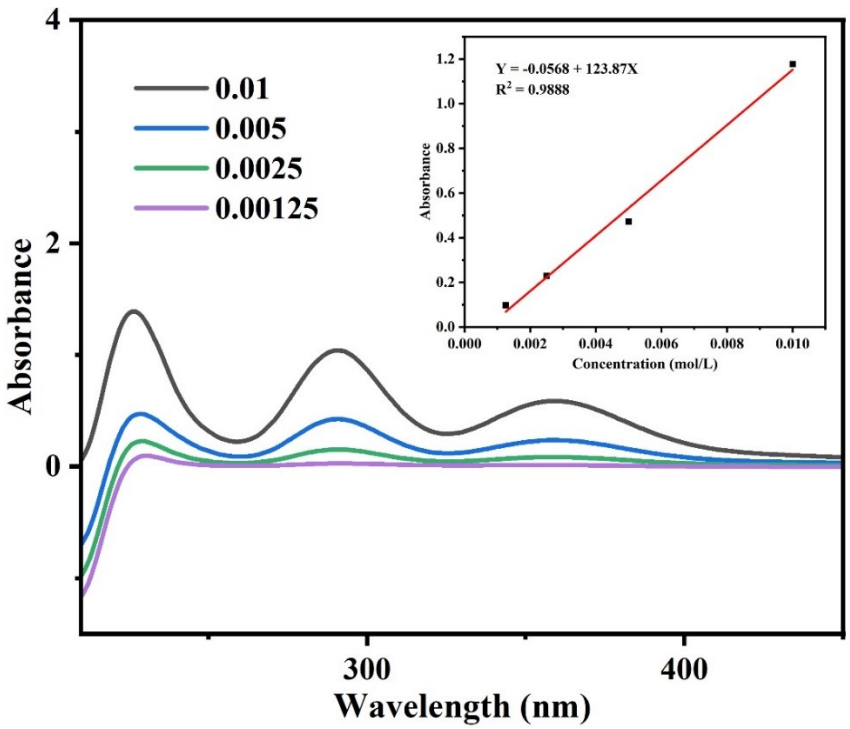

Fig. S5 UV spectra of methanol standard solution of iodine.

Table S4. The iodine desorption rate of I_2@Cd-MOFs.

	absorbance intensity	desorption of I_2 (g)	adsorption of I_2 (g)	recovery rate
I_2@HSB-W8	0.02327	0.00328	0.00349	93.98%
I_2@HSB-W9	0.01933	0.00312	0.00329	94.83%

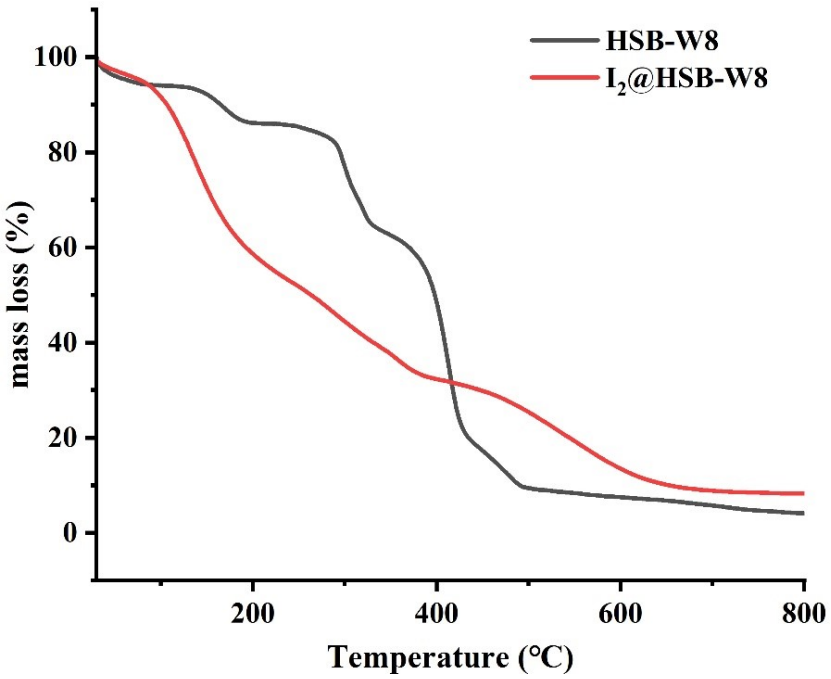

Fig. S6 TGA plots for HSB-W8 and I_2@HSB-W8.

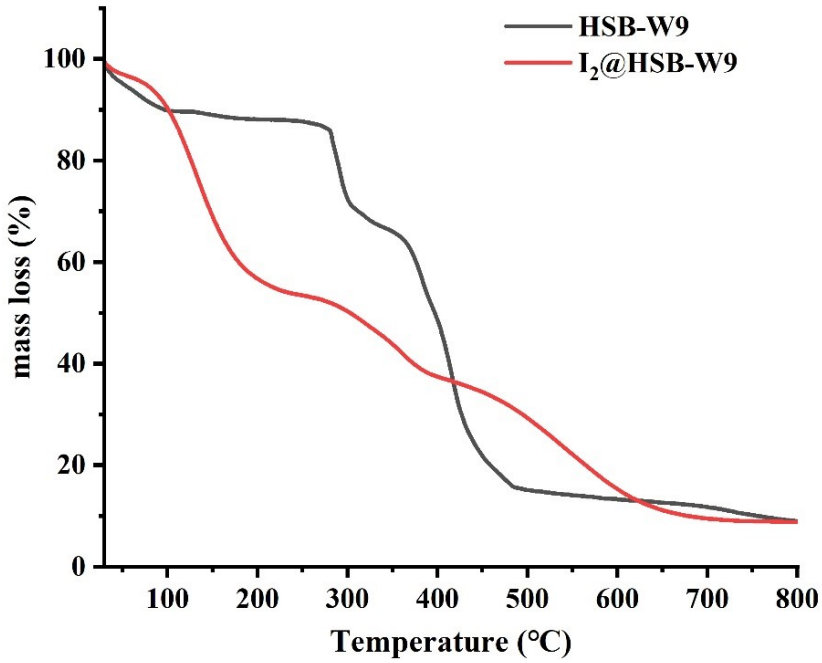

Fig. S7 TGA plots for HSB-W9 and I_2@HSB-W9.

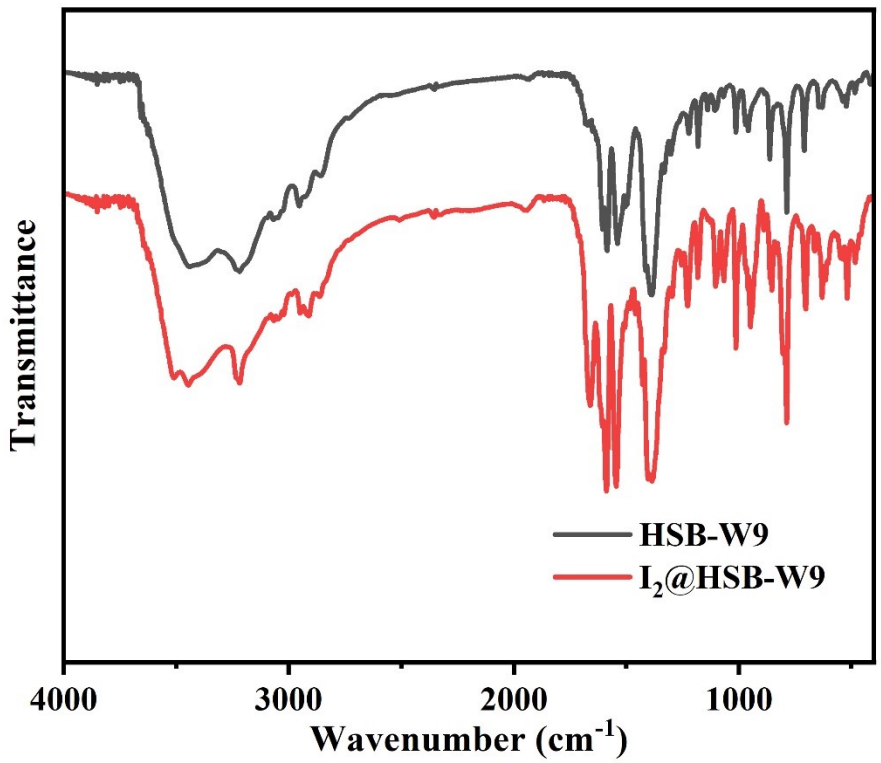

Fig. S8 FT-IR spectra of HSB-W9 and I_2@HSB-W9.

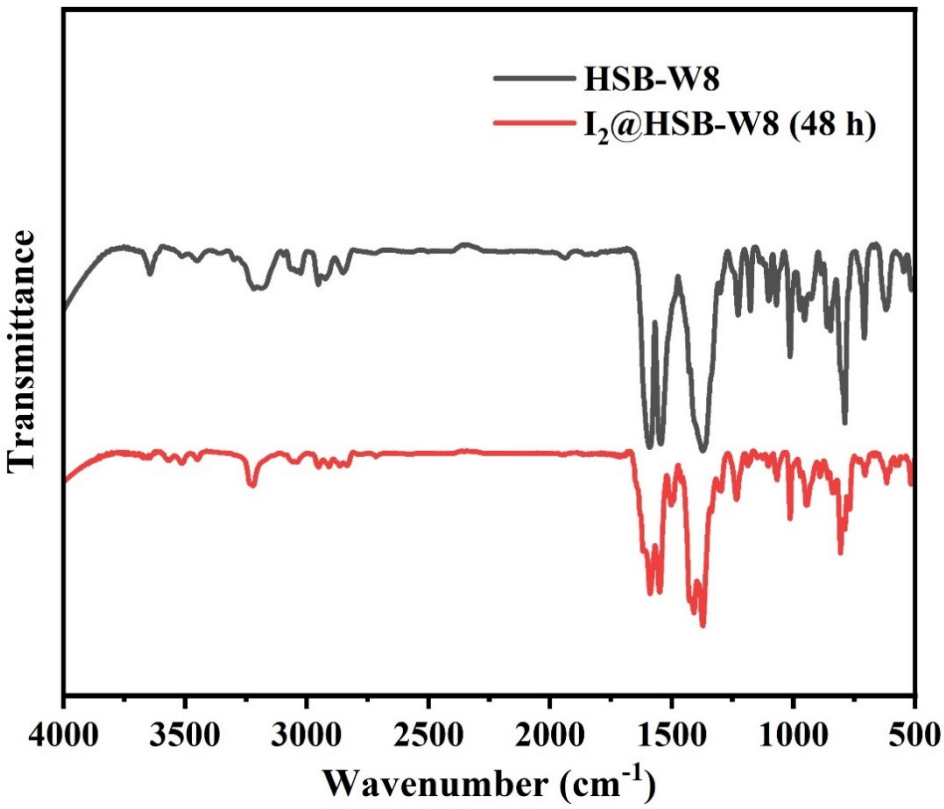

Fig. S9 FT-IR spectra of HSB-W8 and I_2@HSB-W8.

Table S5. The calculated adsorption energy of I_2 molecules interacts with the carbon-

Adsorption energy (eV)	HSB-W8 + I_2	HSB-W9 + I_2
Carbon-Carbon double bonds	-1.24	-0.36
N atoms	0.6	0.26

carbon double bond of stilbene and secondary amine of hsb-2.

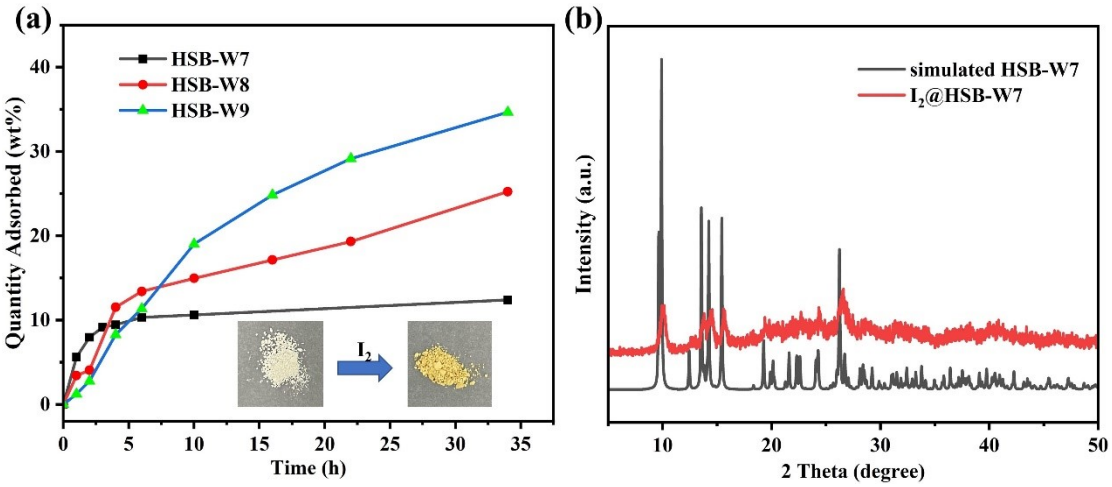

Fig. S10 (a) Comparison of the adsorption capacity of HSB-W7, HSB-W8 and HSB-W9 at 25°C in iodine vapor. Inset is the color evolution of the HSB-W7 before and after I_2 uptake. (b) PXRD patterns of I_2@HSB-W7.

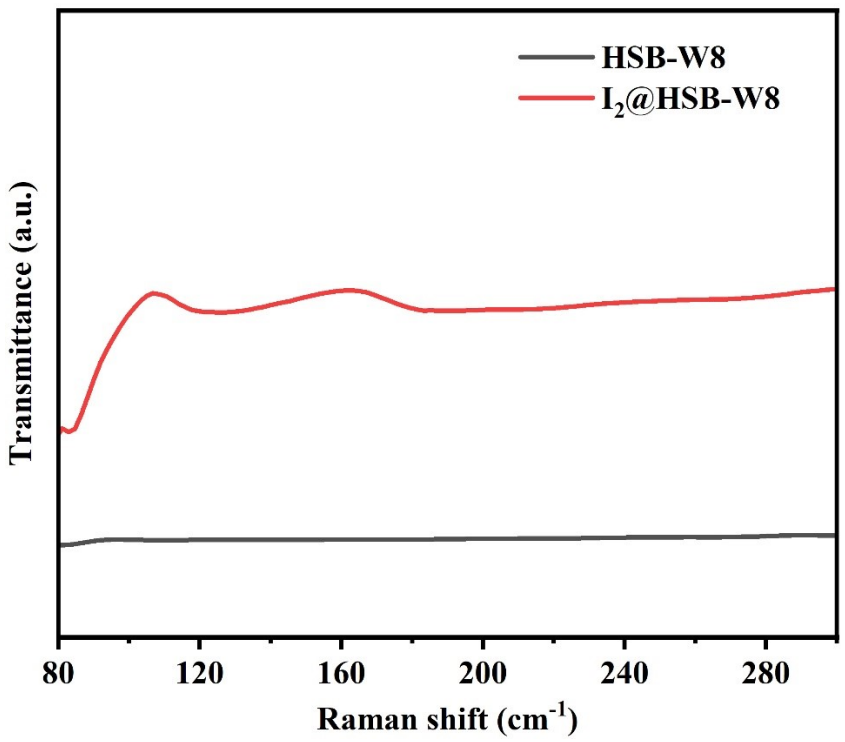

Fig. S11 Raman spectra of HSB-W8 and I_2@HSB-W8.

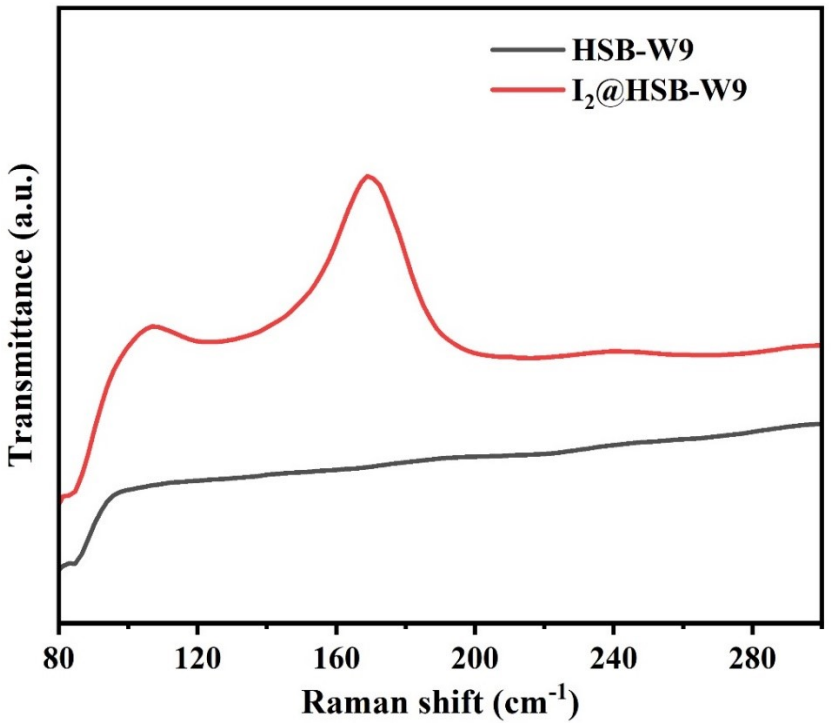

Fig. S12 Raman spectra of HSB-W9 and I_2@HSB-W9.

Computational details：

DFT calculations were performed as implemented in the Vienna ab initio simulation package (VASP).[32,33] The projector augmented wave (PAW) method was adopted to describe interactions between ions and electrons.[34] The generalized gradient approximation (GGA) in the form of Perdew, Burke, Ernzerhof (PBE) was used to describe electron exchange and correlation.[35] The plane-wave basis set along with a kinetic cutoff energy was 400 eV. The Brillouin zones were sampled with 3 × 3 × 1 Monkhorst-Pack meshes. The structures were fully relaxed until the maximum force on each atom was less than –0.02 eV/Å and 10-5 eV. The van der Waals interaction was considered using the DFT-D3 scheme.

REFERENCES

[1] N. Liu, J. Chen, Z. Wu, P. Zhan, L. Zhang, Q. Wei, F. Wang and L. Shao, Construction of Microporous Lignin-Based Hypercross-Linked Polymers with High Surface Areas for Enhanced Iodine Capture, *ACS Appl. Poly. Mater.,* 2021, ***3***, 2178-2188.

[2] P. Chen, X. He, M. Pang, X. Dong, S. Zhao and W. Zhang, Iodine Capture Using Zr-Based Metal-Organic Frameworks (Zr-MOFs): Adsorption Performance and Mechanism, *ACS Appl. Mater. Interfaces,* 2020, ***12***, 20429-20439.

[3] Y. Tang, H. Huang, J. Li, W. Xue and C. Zhong, IL-induced formation of dynamic complex iodide anions in IL@MOF composites for efficient iodine capture, *J. Mater. Chem. A*, 2019, ***7***, 18324-18329.

[4] D. Chen, Y. Fu, W. Yu, G. Yu and C. Pan, Versatile Adamantane-based porous polymers with enhanced microporosity for efficient CO_2 capture and iodine removal, *Chem. Eng. J.,* 2018, ***334***, 900-906.

[5] X. Chen, X. Jiang, X. Lei, B. Zhang, M. Qiao, C. Yin and Q. Zhang, Direct Synthesis of Two-Dimensional Metal–Organic Framework Nanoplates for Noble Metal Load and Gaseous Iodine Adsorption, *Cryst. Growth Des.,* 2020, ***20***, 1378-1382.

[6] A. Gogia, P. Das and S. K. Mandal, Tunable Strategies Involving Flexibility and Angularity of Dual Linkers for a 3D Metal-Organic Framework Capable of Multimedia Iodine Capture, *ACS Appl. Mater. Interfaces,* 2020, ***12***, 46107-46118.

[7] D. F. Sava, M. A. Rodriguez, K. W. Chapman, P. J. Chupas, J. A. Greathouse, P. S. Crozier and T. M. Nenoff, Capture of volatile iodine, a gaseous fission product, by zeolitic imidazolate framework-8, *J. Am. Chem. Soc.,* 2011, ***133***, 12398-12401.

[8] B. Qi, Y. Liu, T. Zheng, Q. Gao, X. Yan, Y. Jiao and Y. Yang, Highly efficient capture of iodine by Cu/MIL-101, *J. Solid State Chem*., 2018, ***258***, 49-55.

[9] X. Zhang, I. D. Silva, H. G. W. Godfrey, S. K. Callear, S. A. Sapchenko, Y. Cheng, I. Vitorica-Yrezabal, M. D. Frogley, G. Cinque, C. C. Tang, C. Giacobbe, C. Dejoie, S. Rudic, A. J. Ramirez-Cuesta, M. A. Denecke, S. Yang and M. Schroder, Confinement of Iodine Molecules into Triple-Helical Chains within Robust Metal-Organic Frameworks, *J. Am. Chem. Soc.,* 2017, ***139***, 16289-16296.

[10] R. J. Marshall, S. L. Griffin, C. Wilson and R. S. Forgan, Stereoselective Halogenation of Integral Unsaturated C-C Bonds in Chemically and Mechanically Robust Zr and Hf MOFs, *Chem. Eur. J.,* 2016, ***22***, 4870-4877.

[11] B. Guo, F. Li, C. Wang, L. Zhang and D. Sun, A rare (3,12)-connected zirconium metal-organic framework with efficient iodine adsorption capacity and pH sensing, *J. Mater. Chem. A*, 2019, ***7***, 13173-13179.

[12] D. Banerjee, X. Chen, S. S. Lobanov, A. M. Plonka, X. Chan, J. A. Daly, T. Kim, P. K. Thallapally and J. B. Parise, Iodine Adsorption in Metal Organic Frameworks in the Presence of Humidity, *ACS Appl. Mater. Interfaces,* 2018, ***10***, 10622-10626.

[13] R. X. Yao, X. Cui, X. X. Jia, F. Q. Zhang and X. M. Zhang, A Luminescent Zinc(II) Metal-Organic Framework (MOF) with Conjugated π-Electron Ligand for High Iodine Capture and Nitro-Explosive Detection, *Inorg. Chem.,* 2016, ***55***, 9270-9275.

[14] G. Brunet, D. A. Safin, M. Z. Aghaji, K. Robeyns, I. Korobkov, T. K. Woo and M. Murugesu, Stepwise crystallographic visualization of dynamic guest binding in a nanoporous framework, *Chem. Sci.,* 2017, ***8***, 3171-3177.

[15] G. Mehlana, G. Ramon and S. A. Bourne, A 4-fold interpenetrated diamondoid metal-organic framework with large channels exhibiting solvent sorption properties and high iodine capture, *Microporous and Mesoporous Mater.,* 2016, ***231***, 21-30.

[16] C. Falaise, C. Volkringer, J. Facqueur, T. Bousquet, L. Gasnot and T. Loiseau, Capture of iodine in highly stable metal-organic frameworks: a systematic study, *Chem. Commun.,* 2013, ***49***, 10320-10322.

[17] Z. Wang, Y. Huang, J. Yang, Y. Li, Q. Zhuang and J. Gu, The water-based synthesis of chemically stable Zr-based MOFs using pyridine-containing ligands and their exceptionally high adsorption capacity for iodine, *Dalton Trans.,* 2017, ***46***, 7412-7420.

[18] L. Hashemi and A. Morsali, Microwave assisted synthesis of a new lead(ii) porous three-dimensional coordination polymer: study of nanostructured size effect on high iodide adsorption affinity, *CrystEngComm,* 2012, ***14***, 779-781.

[19] M.-H. Zeng, Q.-X. Wang, Y.-X. Tan, S. Hu, H.-X. Zhao, L.-S. Long and M. Kurmoo, Rigid Pillars and Double Walls in a Porous Metal-Organic Framework: Single-Crystal to Single-Crystal, Controlled Uptake and Release of Iodine and Electrical Conductivity, *J. Am. Chem. Soc.,* 2010, ***132***, 2561-2563.

[20] G. Massasso, J. Long, J. Haines, S. Devautour-Vinot, G. Maurin, A. Grandjean, B. Onida, B. Donnadieu, J. Larionova, C. Guerin and Y. Guari, Iodine capture by Hofmann-Type clathrate $Ni^{II}(pz)[Ni^{II}(CN)_4]$, *Inorg. Chem.,* 2014, ***53***, 4269-4271.

[21] A. K. Chaudhari, S. Mukherjee, S. S. Nagarkar, B. Joarder and S. K. Ghosh, Bi-porous metal–organic framework with hydrophilic and hydrophobic channels: selective gas sorption and reversible iodine uptake studies, *CrystEngComm,* 2013, ***15***, 9465-9471.

[22] P. Cui, L. J. Ren, Z. Chen, H. C. Hu, B. Zhao, W. Shi and P. Cheng, Temperature-controlled chiral and achiral copper tetrazolate metal-organic frameworks: syntheses, structures, and I_2 adsorption, *Inorg. Chem.,* 2012, ***51***, 2303-2310.

[23] Q. K. Liu, J. P. Ma and Y. B. Dong, Highly efficient iodine species enriching and guest-driven tunable luminescent properties based on a cadmium(II)-triazole MOF, *Chem. Commun.,* 2011, ***47***, 7185-7187.

[24] V. Safarifard and A. Morsali, Influence of an amine group on the highly efficient reversible adsorption of iodine in two novel isoreticular interpenetrated pillared-layer microporous metal–organic frameworks, *CrystEngComm,* 2014, ***16***, 8660-8663.

[25] S. Parshamoni, S. Sanda, H. S. Jena and S. Konar, Tuning CO_2 uptake and reversible iodine adsorption in two isoreticular MOFs through ligand functionalization, *Chem.-Asian J.,* 2015, *10*, 653-660.

[26] M. Liu, W. Liao, C. Hu, S. Du and H. Zhang, Calixarene-based nanoscale coordination cages, *Angew. Chem., Int. Ed.,* 2012, ***51***, 1585-1588.

[27] A. S. Munn, F. Millange, M. Frigoli, N. Guillou, C. Falaise, V. Stevenson, C. Volkringer, T. Loiseau, G. Cibin and R. I. Walton, Iodine sequestration by thiol-modified MIL-53(Al), *CrystEngComm,* 2016, ***18***, 8108-8114.

[28] S. Yao, X. Sun, B. Liu, R. Krishna, G. Li, Q. Huo and Y. Liu, Two heterovalent copper–organic frameworks with multiple secondary building units: high performance for gas adsorption and separation and I_2 sorption and release, *J. Mater. Chem. A,* 2016, ***4***, 15081-15087.

[29] Y. Rachuri, K. K. Bisht and E. Suresh, Two-Dimensional Coordination Polymers Comprising Mixed Tripodal Ligands for Selective Colorimetric Detection of Water and Iodine Capture, *Cryst. Growth Des.,* 2014, ***14***, 3300-3308.

[30] F. Sun, Z. Yin, Q. Q. Wang, D. Sun, M. H. Zeng and M. Kurmoo, Tandem postsynthetic modification of a metal-organic framework by thermal elimination and subsequent bromination: effects on absorption properties and photoluminescence, *Angew. Chem., Int. Ed.,* 2013, ***52***, 4538-4543.

[31] J. Wang, J. H. Luo, X. L. Luo, J. Zhao, D.-S. Li, G. H. Li, Q. S. Huo and Y. L. Liu, Assembly of a Three-Dimensional Metal–Organic Framework with Copper(I)

Iodide and 4-(Pyrimidin-5-yl) Benzoic Acid: Controlled Uptake and Release of Iodine, *Cryst. Growth Des.,* 2015, ***15***, 915-920.

[32] G. Kresse and J. Hafner, Ab initio molecular-dynamics simulation of the liquid metals, *Phys. Rev. B*, 1993, ***47***, 558.

[33] G. Kresse and J. Furthmüller, Efficiency of ab-initio total energy calculations for metals and semiconductors using a planewave basis set, *Comput. Mater. Sci*., 1996, ***6***, 15-50.

[34] P. E. Blöchl, Projector augmented-wave method, *Phys. Rev. B: Condens. Matter Mater. Phys*., 1994, ***50***, 17953.

[35] J. P. Perdew, K. Burke and M. Ernzerhof, Generalized Gradient Approximation Made Simple, *Phys. Rev. Lett.*, 1996, ***77***, 3865-3868.